Molecular-dynamics investigation of orientational freezing in solid C_{60}

Ailan Cheng and Michael L. Klein
Department of Chemistry, University of Pennsylvania, Philadelphia, Pennsylvania 19104-6323 and Laboratory for Research on the Structure of Matter, University of Pennsylvania, Philadelphia, Pennsylvania 19104-6323
(Received 30 August 1991)

Constant-pressure molecular-dynamics calculations have been carried out to investigate the reorientational behavior of C_{60} molecules in the solid phase. Under ambient conditions, an intermolecular potential based on pairwise-additive atom-atom interactions yields a stable fcc crystal in which the C_{60} molecules are found to undergo rotational diffusion. On cooling to 200 K the molecules freeze into an orientational ordered structure with tetragonal symmetry. Although the presence of a phase transition just below room temperature agrees well with calorimetric, x-ray, and NMR data, the predicted low-temperature structure does not. Possible reasons for this are discussed. The orientational relaxation time and phonon density of states are calculated at several temperatures. The former is in fair agreement with NMR data.

I. INTRODUCTION

The discovery of the carbon cluster C_{60} has opened a horizon for scientists from many disciplines.[1] It is known that the 60 carbon atoms in the cluster sit on the vertices of a truncated icosahedron, and hence from a soccer-ball-like molecule called fullerene.[1] The effective synthesis of fullerene[2] has made it possible to study the traditional solid-state properties of this new form of carbon and to study its chemistry. The recent observation of superconductivity in the alkali-metal-doped solids (fullerides) has attracted considerable attention.[3–8]

Experimental techniques such as nuclear-magnetic-resonance (NMR),[9–11] x-ray-diffraction,[12–15] and theoretical methods,[16–19] such as static energy minimization[18] and molecular-dynamics solution,[19] have been used to investigate the structure and orientational properties of this fascinating system. The x-ray studies indicate that under ambient conditions pure C_{60} solid is a face-centered-cubic (fcc) crystal in which the fullerene molecules undergo rotational diffusion.[9–12] The NMR (Ref. 11) and calorimetrical measurements[12] suggest that a phase transition occurs on cooling to around 260 K, while the x-ray study suggests 249 K.[12] High-pressure and infrared spectroscopic data indicate a transition to a low-symmetry phase.[20,21] In this article, we present molecular-dynamics results for pure solid C_{60} based on a pairwise-additive atom-atom intermolecular potential. Anticipating results we will see that this simple model is able to rationalize some, but not all, of the available data.

II. DETAILS OF THE CALCULATIONS

Molecular-dynamics calculation have been performed using a rigid molecule description, since the high-frequency intramolecular vibrations couple weakly with molecular thermal motion. As mentioned above, the 60 carbon atoms of fullerene form a truncated icosahedron, which consists of 12 pentagonal and 20 quasihexagonal faces. There are two distinct C-C bond lengths. The values used in this work, 1.37 and 1.448 Å, were taken from the quantum-chemistry calculations.[22] Intermolecular interactions were represented by a C-C Lennard-Jones (12-6) potential with the parameters ($\varepsilon=28$ K and $\sigma=3.4$ Å) taken from a study of graphite.[23] The C-C potential obtained from a recent intermolecular potential fitting[24] to the lattice spacing and heat of sublimation[25] of pure C_{60} solid is very similar to the potential used herein. We have shown elsewhere[19] that the calculated lattice constant as a function of pressure is in fair agreement with the experimental equation of state up to 20 kbar.[14,20]

Due to the large number of interaction sites on each C_{60}, most of the molecular-dynamics simulations were performed on a small system with $2\times2\times2$ fcc unit cells. A single calculation was carried out for a periodically replicated fcc lattice with $3\times3\times3$ unit cells for comparison. We employed a constant-pressure algorithm,[26,27] which allows volume and shape fluctuations of the simulation box. The required Parrinello-Rahman equations of motion for the translational degrees of freedom were solved by using a third-order Gear predictor-corrector algorithm.[28] The rotational degrees of freedom, described by quaternions, were intergrated by a fourth-order algorithm. Typically systems are allowed to relax for about 30 ps, after which configurations were collected to determine ensemble averages of various properties.

Since the C_{60} molecule has icosahedral symmetry, orientational ordering is described by appropriate averages of the spherical harmonic functions of sixth order, $\langle[Q_{6m}]\rangle=\langle[\sum Y_{6m}]_{\rm av}\rangle$, where $m=0,1,\ldots,6$. The summation is over the 60 carbon atoms on each molecule, $[\cdots]$ denotes an ensemble average, and $\langle\cdots\rangle$ represents an average over all molecules. Analytical expressions for the Y_{6m} are given in the Appendix. There are 13 independent "order parameters" corresponding to the real and imaginary parts of each Y_{6m}. For a free rotor, the average $\langle|[\sum Y_{6m}]_{\rm av}|\rangle=0$. When the Bucky

ball is oriented with a twofold, threefold, or fivefold axis, etc., pointing along crystal axes, certain of the $\langle |[\sum Y_{6m}]_{av}| \rangle$ are large whereas others vanish by symmetry. The values of these order parameters depend on which of the three crystal axes the C_{60} symmetry axes aligned along. The values for several ideal orientations are presented (see Table II in the Appendix).

III. SIMULATION RESULTS

A. Atom-atom model

Molecular-dynamics calculations were performed at zero pressure for several temperatures ranging from 350 down to 80 K in order to study orientational freezing. Throughout the run carried out under ambient conditions, the crystal structure of solid C_{60} remained face centered cubic. The calculated lattice constant 14.14 Å agreed well with the experimental value of 14.17 Å.[12] In this structure the fullerene molecules are rotating as is indicated in Fig. 1, which is a snapshot of the typical orientational-disordered configuration. The calculated configurational energy, volume, and enthalpy are given in Table I.

Orientational freezing can be monitored by following the variation of the rotational diffusion coefficients with temperature.[19] However, microscopic orientational order is better described by following the temperature variation of the quantities $\langle |[\sum Y_{6m}]_{av}| \rangle$, defined in the Appendix. Values calculated from the molecular-dynamics trajectories are shown in Fig. 2. At high temperature the order parameters are small, and suggest that the C_{60} molecules behave like weakly hindered rotors. The rapid change of some order parameters below 200 K indicates that C_{60} molecules have stopped rotating on the simulation time scale. Furthermore, the large values for $\mathrm{Re}\langle |[\sum Y_{6m}]_{av}| \rangle$, $m=0,4$ and $\mathrm{Im}\langle |[\sum Y_{6m}]_{av}| \rangle$, $m=2,6$, and nearly zero values for other m at low temperature are indicative of freezing into a well-defined order phase.

The nature of the ordering is clear in the snapshot of the configuration at 106 K shown in Fig. 3. The orientations of three mutually perpendicular twofold axes of the Bucky ball point in the following way. One of these twofold axis points along a crystal axis, in this case the z axis, and the remaining two axes point along [110] and [$\bar{1}$10] directions, respectively. Since these two twofold axes are not equivalent, there exist two distinct molecular orientations, which differ by a 90° rotation. (These occur with equal probability.) The small system size studied here, and existence of some defects (misoriented molecules), makes it difficult to define the unit cell of the lattice. With the kind of molecular orientational ordering mentioned above, some of the molecular hexagonal faces stay parallel with those of neighboring molecules, but the centers of these two hexagons are displaced relative to each other similar to that in the local structure between two graphite sheets. The hexagonal faces are inclined 36° away from the first twofold axis. This kind of relative orientation can be better accommodated if the crystal lattice undergoes a tetragonal distortion, as shown in Fig. 4. The packing of C_{60} molecules is no longer equivalent along the x, y, and z directions.

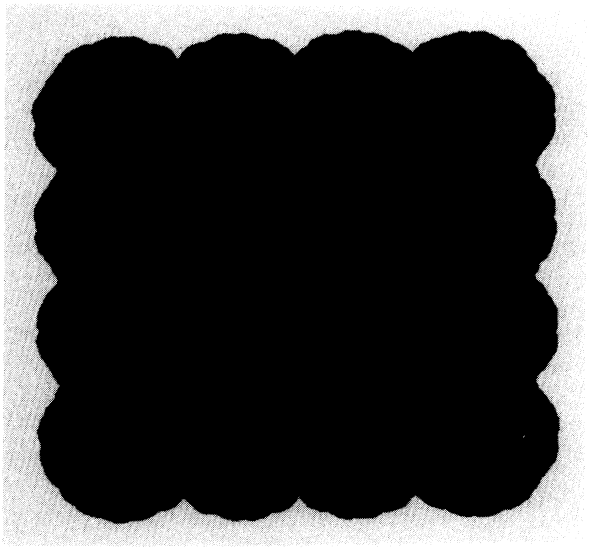

FIG. 1. A snapshot of C_{60} molecules in the fcc rotator phase at 340 K (see text).

We have also carried out a simulation at 103 K for a system containing 108 C_{60} molecules, primarily in order to obtain more information on phonon modes. Both the resulting structure and the orientational information are consistent with the small system results. The orientational order parameters, and lattice constants are shown in

TABLE I. Molecular-dynamics results.

N	T (K)	U_{conf} (kJ/mol)	V (Å^3/molecule)	H (kJ/mol)	τ (ps)
32	83.4	−153.5	686.8	−151.3	
	106.0	−153.4	687.1	−150.6	1136
	157.6	−150.7	692.0	−146.5	195
	202.0	−146.9	699.0	−141.7	20
	266.7	−145.0	702.8	−138.1	15
	256.2	−144.5	703.8	−137.8	
	267.9	−144.7	703.5	−137.8	
	340.3	−142.2	706.4	−133.5	5
108	103.1	−152.9	694.5	−150.3	

the figures together with data of the smaller systems.

Simulations at room temperature and two pressures, $P=75$ and 150 kbar, indicated that the structure and the orientational ordering of the solid are very similar to that of the low-temperature phase, except that the lattice constant is much smaller. As in the low-temperature phase, the lattice distorted away from being cubic, but with unit-cell lengths $a=b=13.6$ Å, $c=12.85$ Å for $P=75$ kbar, and $a=b=13.4$ Å, $c=12.65$ Å for $P=150$ kbar. This predicted orientational ordered phase may correspond to the low symmetry phase observed in the recently reported experiments at high pressure.[21] The calculated average lattice constant is compared with experimental compression data[14,20] in Fig. 5. It seems that the 12-6 C-C potential is slightly too hard in the high-pressure region. This may be due in part to the use of a rigid molecule. A recent calculation based on a flexible model predicts a distortion of the C_{60} structure at high pressure.[29]

Molecular reorientation can be studied by calculating the autocorrelation functions (ACF's) of unit vectors along symmetry axes. For simplicity we focus here on the twofold axes. A fit of the long-time tail of the correlation function to an exponential form yields reorientational times, which are listed in Table I. A dramatic increase of reorientational time accompanies the freezing of C_{60} molecules. Indeed, at low temperatures the estimated times greatly exceed the MD run lengths and are hence subject to large uncertainty. The relaxation time, especially in the low-temperature region, is much shorter than that estimated from NMR data[11] and neutron scattering.[30] Orientation of a body-fixed c_2 axis relative to a reference frame changes even when molecules jump to equivalent orientations. Thus, the calculated relaxation time herein is different from that obtained in quasielastic neutron scattering, and is usually shorter. However, x-ray and neutron measurements cannot detect the difference between equivalent orientations. Taking this fact into account, we calculated ACF's of order parameters, $Q_{6m}=\sum Y_{6m}$, which are invariant when molecules rotate to equivalent orientations. Figure 6 shows the variation with temperature of the Q_{6m} ACF for $m=4$. Clearly, a slowing down in the reorientational motion sets in below 200 K. The oscillation in the short-time region indicates librational motion with a period of about 3 ps, which yields about 11 cm^{-1} for the librational frequency. This estimate is consistent with that obtained from the angular velocity ACF (see below). The relaxation time obtained from autocorrelation of order parameters in the room-temperature range agree well with both NMR data and the above-mentioned calculation. In the low-temperature range it is not very easy to estimate a relaxation time because of the inevitable poor statistics in the long-time region. The short relaxation time obtained from the ACF of c_2 may result from several facts. First of all, due to the slow reorientation at low temperature, it is really necessary to have a longer simulation run to obtain a meaningful long-time tail. Therefore, the calculated relaxation times gives a lower limit. Also, the time-dependent configurations displayed on a graphics terminal indicate that one of 32 C_{60} molecules rotates rather fast even at low temperature. This makes the average relaxation time shorter. Third, the discrepancy is likely due to the fact that the potential barrier for the orientational motion in the model is too low. A lower barrier

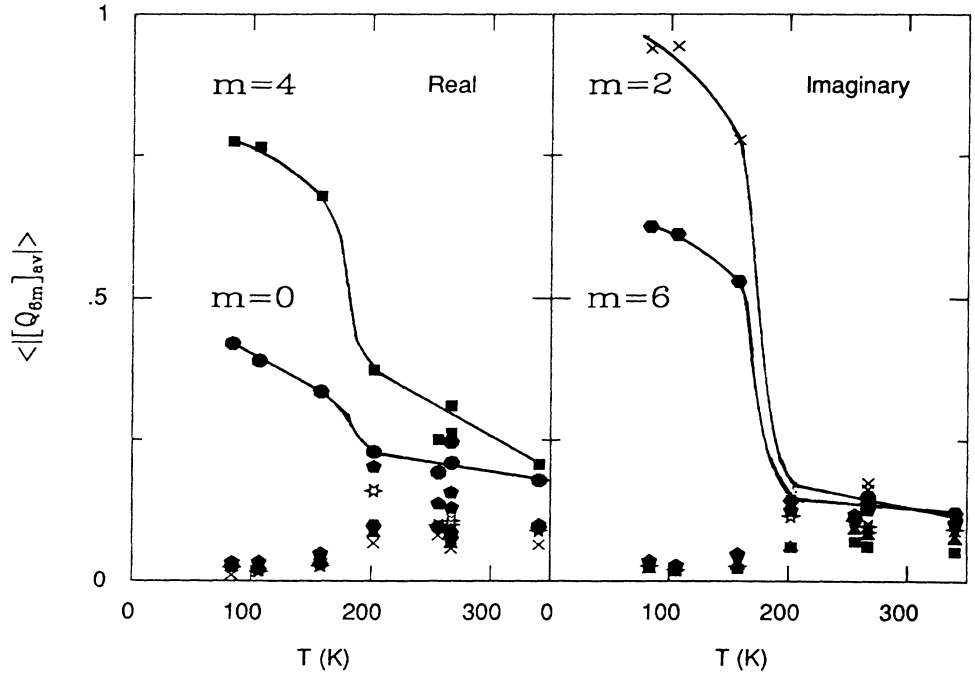

FIG. 2. Orientational order parameters $\langle|[\sum Y_{6m}]_{av}|\rangle$, as defined in the text. Solid circles, $m=0$; asterisks, $m=1$; crosses, $m=2$; triangles, $m=3$; squares, $m=4$; pentagons, $m=5$; and hexagons, $m=6$. The abrupt change of the calculated values below 200 K signals the onset of orientational freezing on the MD time scale. Solid lines are a guide to the eye.

height inevitably permits the C_{60} molecule to rotate faster.

The density of phonon states has been obtained from the ACF's of velocity and angular velocity. Figure 7 shows the Fourier transformation of the average values of ACF's for a $2\times2\times2$ fcc lattice at 106 K and a $3\times3\times3$ system at 103 K. It is clear that in solid C_{60} the librational motions have much lower frequencies than the translational modes. Some phonon peaks are split at low temperature due to the distortion of the lattice from a cubic structure. Application of pressure causes the density of phonon states to shift to much higher frequency as shown in Fig. 8. The high-pressure librational modes shift to 40 cm^{-1} from a value of 10 cm^{-1}, in the low-temperature ordered phase. Both the average frequency of the translational band and the bandwidth are almost triple the zero-pressure values.

B. Local quadrupole model

In the model used above, the low-temperature structure obtained in the simulation arises from an efficient packing of molecules. In an attempt to reproduce the low-temperature structure proposed on the basis of experimental data[12] and to raise the transition temperature,

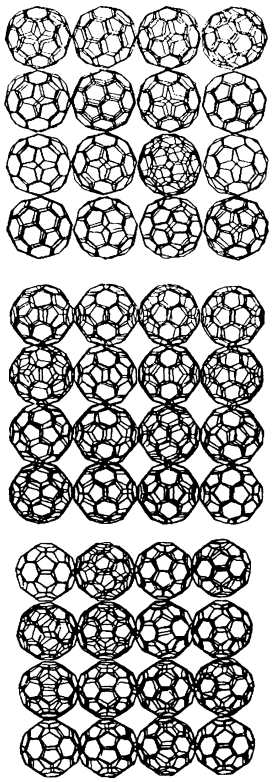

FIG. 3. Snapshot of a configuration viewed from three orthogonal directions for a $2\times2\times2$ fcc lattice at 106 K showing the predicted ordering of the C_{60} molecules. Each panel in the figure is the superposition of four molecular planes. Therefore, the snapshot appears to be a simple cubic lattice. The parallel alignment of quasihexagonal faces of adjacent molecules can be seen in the y-z (middle) and x-z (lower) planes.

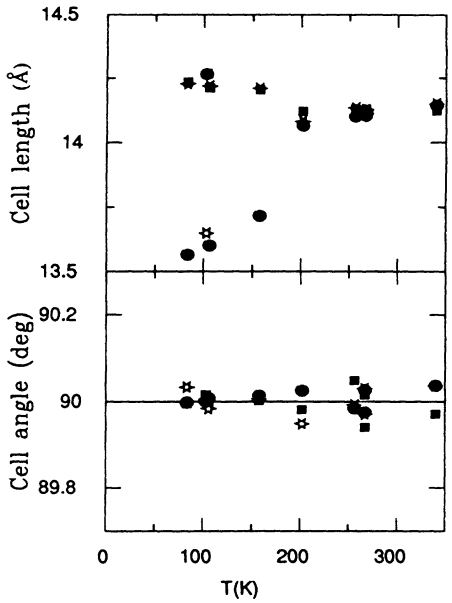

FIG. 4. Variation of the equivalent fcc cell lengths and angles with temperature. The cell distortion around 200 K coincides with the onset of orientational freezing. Note that the cell angles stay at 90°.

we have also carried out simulations with a modified potential model. Several aromatic molecules, such as benzene, napthalene, and anthracene, have very considerable quadrupole moments. Also, C_{60} is an aromatic molecule whose hexagonal faces are somewhat similar to benzene rings. Therefore, a natural first modification of the potential is to include a quadrupole moment for each face. For convenience we will call this the local quadrupole model. A recent study of the benzene-graphite interaction included local quadrupole moments on the graphite basal plane.[31] Since the C_{60} molecule is, in some sense,

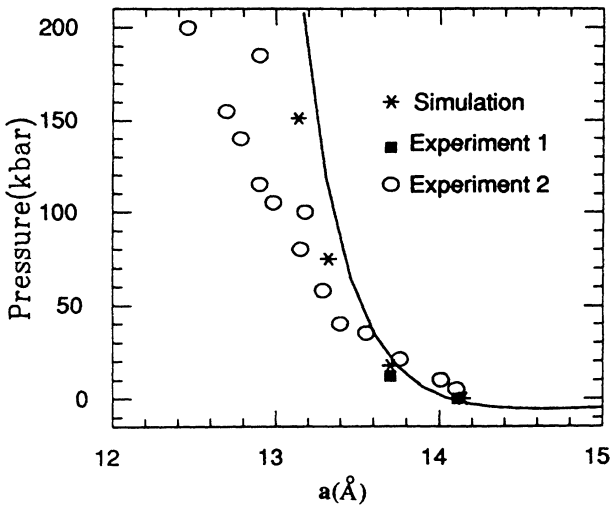

FIG. 5. Average lattice parameter as a function of pressure from static energy (solid line) and molecular-dynamics calculations compared with experimental data from Ref. 14 (experiment 1) and Ref. 20 (experiment 2).

similar to a fragment of curled graphite sheet, we have used the same idea here. Indeed, the value of quadrupole moment used was taken from benzene-graphite work.[31] In effect, we assume that in the three materials mentioned above the component of a quadrupole moment per carbon atom perpendicular to the molecular plane is constant. Accordingly, a quadrupole moment of -1.32 B is assigned on each carbon along the radial direction. For the convenience of calculation, we have used a fractional charge representation. Thus, a charge of $0.56e$ is placed at each carbon atom and two charges of $-0.28e$ are placed 0.7 Å from each carbon along the radial direction, one inside the C_{60} molecule and another outside. With this kind of charge distribution, the net quadrupole moment of the whole C_{60} molecule is, of course, zero due to the symmetry. However, the local charges raise potential barriers for the rotational motion dramatically. The barrier now ranges from 1000 to 3000 K, depending on the relative orientations of a pair of C_{60} molecules compared with 30 to 500 K in the original model.

The local quadrupole model yields very reasonable high-temperature properties. In particular, the calculated lattice constant at room temperature, 14.4 Å, agrees with the experimental value to within 2%. The configurational energy is now less than 10% greater than the measured heat of sublimation.[25] Due to the enhanced potential barrier for the rotational motion, reorientations are slower than that from the simple atom-atom model. The competition between electrostatic and van der Waals interaction results in a different orientational ordering compared with the previous simulation where the ordering is dominated by atomic packing considerations. However, at low temperature, the lattice again underwent a tetragonal distortion, but with $a=b=14.1$ Å and $c=14.4$ Å at $T=100$ K. Though the barriers are higher, the competition between the two types of interactions did not help to raise the transition temperature. Thus, it seems that this local quadrupole model is unlikely to reconcile the difference between experimental data and the results from the simple potential for the pure C_{60} system.

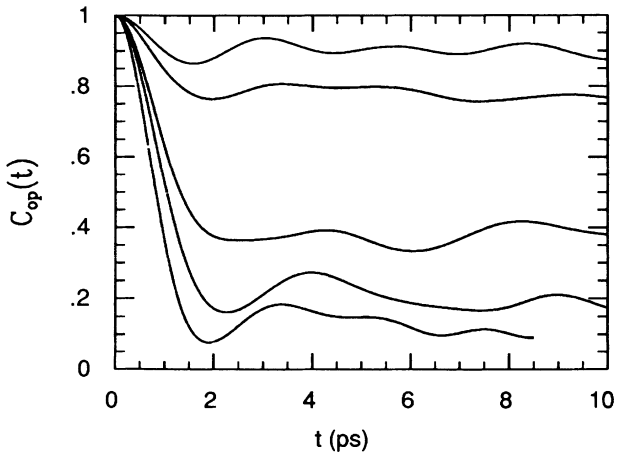

FIG. 6. Autocorrelation function of Q_{6m} for $m=4$. From top to bottom, curves are for $T=106$, 157, 202, 256, and 340 K, respectively.

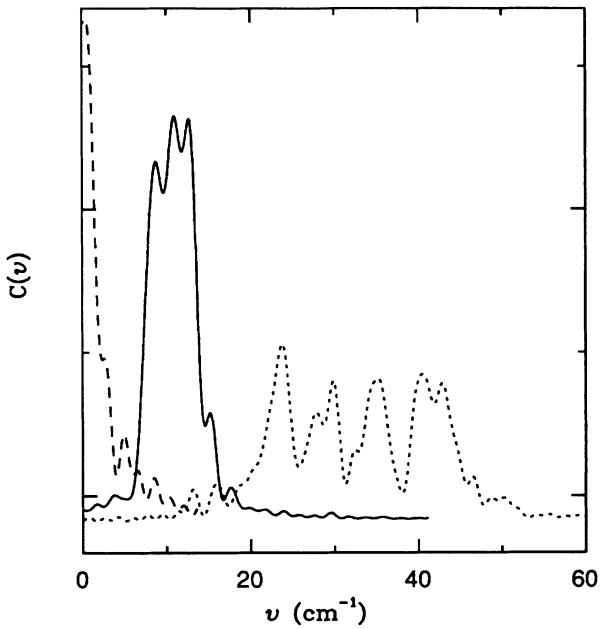

FIG. 7. Lattice vibrations of solid C_{60}. Shown are averaged power spectra from VACF's for a $2\times2\times2$ lattice at 106 K and a $3\times3\times3$ lattice at 103 K. The dotted and solid curves are for translational and librational motion, respectively. Dashed line is the power spectrum of C_{60} librational modes at 340 K.

IV. CONCLUSIONS

Computer simulations have been carried out to investigate the orientational ordering of molecules in solid C_{60}. Two different potential models give reasonable room-temperature properties. Also, the calculated lattice con-

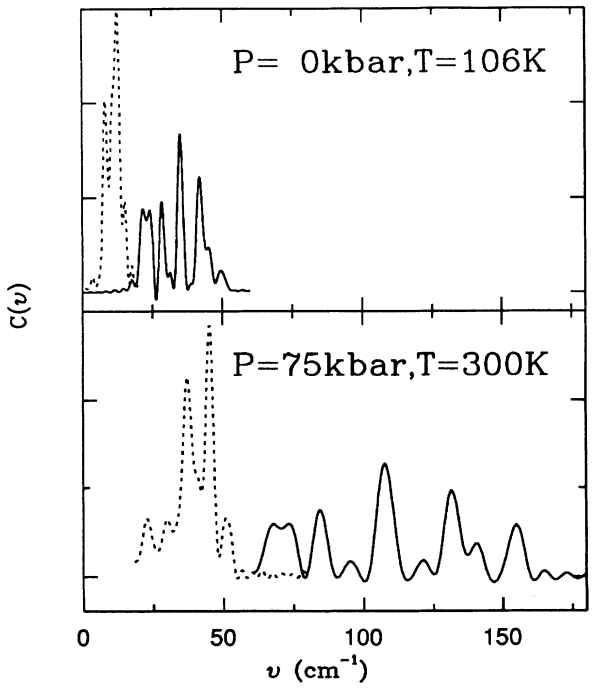

FIG. 8. Room-temperature density of states for a $2\times2\times2$ lattice at zero pressure and $P=75$ kbar. Solid and dotted curves are for translational and librational motions, respectively.

stant as a function of pressure agrees well with experiment in the low-pressure region. The calculated density of phonon states provides rudimentary information on the dynamics of the solid, which remains to be tested by appropriate experiments. The simulation results indicate that there exists a transition from a hindered rotor to an orientationally ordered phase as temperature decreases. This is consistent with experimental findings.[11–13] However, the calculated transition temperature is lower than the experimental value and the predicted tetragonal distortion is not observed in the x-ray experiments.[12] The discrepancies between experiments and the simulation data most likely result from the oversimplified intermolecular pair-potential models. As shown in Table I, the calculated potential energy of the solid is less than the measured heat of sublimation.[25] A rescaling of the C-C well depth by 15% would likely improve the agreement with the experimental transition temperature somewhat but is unlikely to alter the ground-state structure.

The low-temperature crystal structure and molecular orientation reported herein are consistent with a recent static calculation which included the internal degrees of freedom of C_{60}.[18] The rigid-molecule description has provided similar structural and orientational information as the flexible-molecule model, at least at low pressure. Since our goal here is not centered on the internal vibrations of the molecules, we have taken advantage of the rigid-molecule model, which not only saved tremendous computational time but also considerably reduced the complexity of the potential. In summary, the present and previous calculations apparently reveal deficiencies in intermolecular potentials currently in use to describe C_{60} and a rationalization of the reported low-temperature structure does not exist at the present time.

ACKNOWLEDGMENTS

We thank our colleagues at the University of Pennsylvania Laboratory for Research on the Structure of Matter for sharing their results on fullerites. Special thanks go to J. E. Fischer and P. A. Heiney for their insight. We also thank E. J. Mele for his help in selecting the appropriate set of order parameters. This research was supported by the National Science Foundation under Grant No. CHE 87-22481, CHE 88-15130, and DMR 88-19885.

APPENDIX

Since C_{60} has icosahedral symmetry, the lowest nonzero order parameters are spherical harmonic functions of sixth order, Y_{6m}. Here, we use the auxiliary functions $Q_{6m}=\sum Y_{6m}$ as order parameters, where the summation is over all 60 carbon atoms on the C_{60} molecule. If $\vec{r}=(x,y,z,)$ is a vector in the direction of each carbon atom, relative to the center of mass of C_{60}, then the Y_{6m} can be expressed in the following way:

$$Y_{60}=\left[\frac{13}{4\pi}\right]^{0.5}\frac{1}{r^6}\left[\frac{231}{16}z^6-\frac{315}{16}z^4r^2+\frac{105}{16}z^2r^4-\frac{5}{16}r^6\right],$$

$$Y_{61}=\left[\frac{13}{4\pi}\right]^{0.5}\left[\frac{1}{42}\right]^{0.5}\frac{(x+iy)}{r^6}\times\left[\frac{693}{8}z^5-\frac{315}{4}z^3r^2+\frac{105}{8}zr^4\right],$$

$$Y_{62}=\left[\frac{13}{4\pi}\right]^{0.5}\left[\frac{1}{1680}\right]^{0.5}\frac{(x+iy)^2}{r^6}\times\left[\frac{3465}{8}z^4-\frac{945}{4}z^2r^2+\frac{105}{8}r^4\right],$$

$$Y_{63}=\left[\frac{13}{4\pi}\right]^{0.5}\left[\frac{1}{60480}\right]^{0.5}\frac{(x+iy)^3}{r^6}\times\left[\frac{3465}{2}z^3-\frac{945}{2}zr^2\right],$$

$$Y_{64}=\left[\frac{13}{4\pi}\right]^{0.5}\left[\frac{2}{10!}\right]^{0.5}\frac{(x+iy)^4}{r^6}\times\left[\frac{10395}{2}z^2-\frac{945}{2}r^2\right],$$

$$Y_{65}=\left[\frac{13}{4\pi}\right]^{0.5}\left[\frac{1}{11!}\right]^{0.5}\frac{(x+iy)^5}{r^6}(10\,395z),$$

$$Y_{66}=\left[\frac{13}{4\pi}\right]^{0.5}\left[\frac{1}{12!}\right]^{0.5}\frac{(x+iy)^6}{r^6}(10\,395).$$

TABLE II. Values of real and imaginary parts of Q_{6m} for molecular twofold, threefold, and fivefold axes pointing along fcc crystal ⟨001⟩ directions.

	c_2[a]		c_3[b]		c_5[c]	
m	Re	Im	Re	Im	Re	Im
0	−0.456	0.000	−0.812	0.000	1.461	0.000
1	0.000	0.000	0.000	0.000	0.000	0.000
2	1.046	0.000	0.000	0.000	0.000	0.000
3	0.000	0.000	−1.240	0.000	0.000	0.000
4	0.854	0.000	0.000	0.000	0.000	0.000
5	0.000	0.000	0.000	0.000	−1.165	0.000
6	−0.705	0.000	0.748	0.000	0.000	0.000

[a]Three mutually perpendicular c_2 axes point along the x, y, and z direction, respectively,
[b]Threefold axis point along the z direction.
[c]Fivefold axis point along the z direction.

[1]H. W. Kroto, J. R. Heath, S. C. O'Brien, R. F. Curl, and R. E. Smalley, Nature **318**, 162 (1985).
[2]H. Kroto, Science **242**, 1139 (1988); W. Krätschmer, L. D. Lamb, K. Fostiropoulos, and D. R. Huffman, Nature **347**, 354 (1990); W. Krätschmer, K. Fostiropoulos, and D. R. Huffman, Chem Phys. Lett. **170**, 167 (1990).
[3]A. F. Hebard, M. J. Rosseinsky, R. C. Haddon, D. W. Murphy, S. H. Glarum, T. T. M. Palstra, A. P. Ramirez, and A. R. Kortan, Nature **350**, 600 (1991).
[4]M. J. Rosseinsky, A. P. Ramirez, S. H. Glarum, D. W. Murphy, R. C. Haddon, A. F. Hebard, T. T. M. Palstra, A. R. Kortan, S. M. Zahurak, and A. V. Makhija, Phys. Rev. Lett. **66**, 2830 (1991).
[5]O. Zhou, J. E. Fischer, N. Coustel, S. Kycia, Q. Zhu, A. R. McGhie, W. J. Romanow, J. P. McCauley Jr., A. B. Smith III, and D. E. Cox, Nature **351**, 462 (1991).
[6]J. H. Weaver, J. L. Martins, T. Komeda, Y. Chen, T. R. Ohno, G. H. Kroll, N. Troullier, R. E. Haufler, and R. E. Smalley, Phys. Rev. Lett. **66**, 1741 (1991).
[7]P. J. Benning, J. L. Martins, J. H. Weaver, L. P. F. Chibante, and R. E. Smalley, Science **252**, 1417 (1991).
[8]P. W. Stephens, L. Mihaly, P. L. Lee, R. L. Whetten, S.-M. Huang, R. Kaner, F. Diederich, and K. Holczer, Nature **351**, 632 (1991).
[9]C. S. Yannoni, R. D. Johnson, G. Meijer, D. S. Bethune, and J. R. Salem, J. Phys. Chem. **95**, 9 (1991).
[10]R. Tycko, R. C. Haddon, G. Dabbagh, S. H. Glarum, D. C. Douglass, and A. M. Mujsce, J. Phys. Chem. **95**, 518 (1991).
[11]R. Tycko, G. Dabbagh, R. M. Fleming, R. C. Haddon, A. V. Makhija, and S. M. Zahurak, Phys. Rev. Lett. **67**, 1886 (1991).
[12]P. A. Heiney, J. E. Fischer, A. R. McGhie, W. J. Romanow, A. M. Denenstein, J. P. McCauley, Jr., A. B. Smith III, and D. E. Cox, Phys. Rev. Lett. **66**, 2911 (1991).
[13]J. S. Tse, D. D. Klug, D. A. Wilkinson, and Y. P. Handa, Chem. Phys. Lett. (to be published).
[14]J. E. Fischer, P. A. Heiney, A. R. McGhie, W. I. Romanow, A. M. Denenstein, J. P. McCauley, Jr., and A. B. Smith III, Science **252**, 1288 (1991).
[15]R. M. Fleming, T. Siegrist, P. M. Marsh, B. Hessen, A. R. Kortan, D. W. Murphy, R. C. Haddon, R. Tycko, G. Dabbagh, A. M. Mujsce, M. L. Kaplan, and S. M. Zahurak (unpublished).
[16]Q. -M. Zhang, Jae-Yel Yi, and J. Bernholc, Phys. Rev. Lett. **66**, 2633 (1991).
[17]B. P. Feuston, W. Andreoni, M. Parrinello, and E. Clementi, Phys. Rev. B **44**, 4056 (1991).
[18]Y. Guo, N. Karasawa, and W. A. Goddard III, Nature **351**, 464 (1991).
[19]A. Cheng and M. L. Klein, J. Phys. Chem. **95**, 6750 (1991).
[20]S. Duclos, K. Brister, R. C. Haddon, A. R. Kortan, and F. A. Theil, Nature **351**, 380 (1991).
[21]Y. Huang, D. F. R. Gilson, and I. S. Butler, J. Phys. Chem. **95**, 5723 (1991).
[22]G. E. Scuseria, Chem. Phys. Lett. **176**, 423 (1991).
[23]W. A. Steele, *The Interaction of Gases with Solid Surfaces* (Pergamon, New York, 1974).
[24]L. A. Girifalco (unpublished).
[25]C. Pan, M. P. Sampson, Y. Chai, R. H. Hauge, and J. L. Margrave, J. Phys. Chem. **95**, 2944 (1991).
[26]M. Parrinello and A. Rahman, Phys. Rev. Lett. **45**, 1196 (1980); J. Appl. Phys. **52**, 7182 (1981).
[27]S. Nosé and M. L. Klein, Mol. Phys. **50**, 1055 (1983); R. W. Impey, M. Sprik, and M. L. Klein, J. Chem. Phys. **83**, 3638 (1985).
[28]C. W. Gear, *Numerical Initial Value Problems in Ordinary Differential Equations* (Prentice-Hall, Englewood Cliffs, NJ, 1971).
[29]Y. Guo, N. Karasawa, and W. A. Goddard III (unpublished).
[30]D. N. Neumann, J. R. D. Copley, R. L. Cappelletti, W. A. Kamitakahar, J. P. McCailey, Jr., K. M. Creegan, N. Coustel, A. B. Smith III, D. M. Cox, J. E. Fischer, N. C. Maliszewsky, and R. M. Lindstrom (unpublished).
[31]A. V. Vernov and W. A. Steele, Langmuir (to be published).

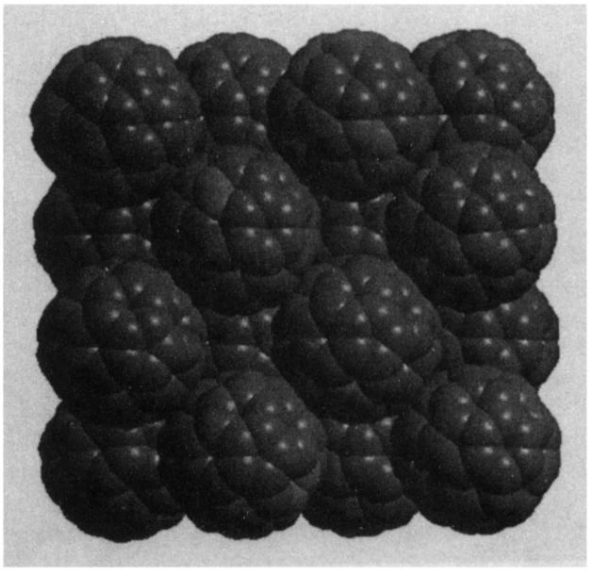

FIG. 1. A snapshot of C_{60} molecules in the fcc rotator phase at 340 K (see text).